condensation," Ber. Deut. Chem. Ges. 68B, 619–624, 1494–1499 (1935).

[3] Kusin, A., "Enolization of sugars under the action of different bases," Ber. Deut. Chem. Ges. 69B, 1041–1049 (1935).

[4] Langenbeck, W., "Formaldehyde condensation as organic autocatalysts. XXII, Organic catalysts," Naturwiss. 30, 30–34 (1942).

[5] Pfeil, E. and Schroth, G., "Kinetics and reaction mechanism of the formaldehyde condensation," Ber. Deut. Chem. Ges. 85, 293–307 (1952).

[6] Pfeil, E. and Ruckert, H., "Formaldehyde condensation. Formation of sugars from formaldehyde by the action of alkalies," Ann. Chem. 641, 121–131 (1961).

[7] Wolford, R. K., "Kinetics of the hydrolysis of acetal in N-methyl-propionamide and N,N-dimethylformamide-water solvents at 20, 25, 30 and 40°," J. Phys. Chem. 67, 632 (1963); also Wolford, R. K. and Bates, R. G., J. Phys. Chem. 66, 1496 (1962).

MAY-JUNE 1964 J. SPACECRAFT VOL. 1, NO. 3

Radiation Shielding Considerations in Manned Spacecraft Design

SIDNEY L. RUSSAK*
The Martin Company, Baltimore, Md.

A procedural analysis that minimizes the space radiation hazard is described for all engineering phases up to hardware design and illustrated by reference to its application in recent studies. Radiation dosages are shown to differ significantly among different spacecraft configurations for the same mission. Estimated radiation dosage levels also vary significantly, depending on the degree of detail to which the spacecraft and body models have been designed. In view of the important mission-configuration-dosage relationships that have been found and the detailed body-radiation tolerances now specified, an efficient treatment of the radiation hazards to manned spaceflight must begin during preliminary design. Detailed inputs must come from system design groups early enough to allow the radiation analysis results to be used in the final determinations of external configuration, materials, and inboard profile.

Introduction

SPACE radiations have received considerable attention during recent years—and have been cited, at various times, as a factor limiting or prohibiting manned space flight, or as being completely insignificant. Depending on the attendant conditions, any of these observations may have been correct.

For a narrower definition of the hazard, we must analyze the characteristics of the mission and the spacecraft in some detail. Such an analysis requires 1) a model of the ambient radiation environment (see the Appendix), 2) a model of the spacecraft or body which interacts with the environment, and 3) the physical relationships that describe the interactions.

Some model environment and spacecraft data will be discussed, not because the data are new but rather to indicate the analytical procedures necessary to the proper consideration of radiations in spacecraft design. At the same time, it is demonstrated that the analysis should begin during the feasibility studies and may well be continued, with expanding detail, in an iterative manner through all of the engineering phases. The analysis requires considerable input data from other technical areas and in turn provides inputs to those areas. It is extremely important that these "feedback" loops be established early.

In this paper, the analytical procedure is discussed for four phases: feasibility studies, preliminary design studies, preliminary design, and design.

Feasibility Studies

The radiation hazard to materials and components is expressed in terms of the incident flux; for man it is usually expressed as dosage absorbed. It is therefore useful to convert the environment from a distribution of particle fluxes to radiation dosage as a function of a standard absorber (a crude representation of the spacecraft). This has been done using several computer programs,[1, 2] which calculate the interactions of the input environment data with the input interacting body data (in this case, hollow spheres of aluminum).

Plots of dose vs aluminum absorber obtained from these programs are shown in Fig. 1 for different constituents of the radiation environment. The effect of orbital parameters on radiation dosages in the Van Allen belts is shown in Fig. 2. The effect of the geomagnetic field in screening out solar flare particles for the May 10, 1959 solar flare is shown in Fig. 3. The proton energy cutoffs used in the preparation of these data were obtained from the solar plasma model of Obayashi and Hakura as given in Ref. 3.

We can now make a first evaluation of the radiation hazard, using as an example a two-week equatorial earth orbit at 600-naut-mile altitude. Table 1 shows a radiation dosage

Table 1 Preliminary estimate of radiation for two-week equatorial orbit at 600 naut miles

Source	Dosage, REM, for aluminum shield thickness, g/cm², 2	6	10
Van Allen belt protons	223	120	85
Secondary neutrons	2	3	4
Van Allen belt electrons	0	0	0
Secondary X-rays	13	9	8
Artificial belt electrons	31,230	0	0
Secondary X-rays	185	159	154
Cosmic rays	~1	~1	~1
Solar flare protons	0	0	0
Total dosage	31,654	292	252

Presented at the AIAA-NASA 2nd Manned Space Flight Meeting, Dallas, Tex. (no preprint number; published in bound volume of preprints of the meeting); revision received January 27, 1964.

* Staff Scientist. Member AIAA.

schedule, within three thicknesses of aluminum, from the various constituents. From this first analysis, it appears that the space radiation would be a significant factor on this mission. If we assume that our spacecraft structure would be at least 6 g/cm² (∼12 lb/ft²), then electrons would not be much of a hazard. If there were any parts of the craft which might be 2 g/cm² or less, then electrons would be a very great hazard. We also see that by 6 g/cm² the x rays are the largest component of dosage. Furthermore, they decrease only a few percent between 6 and 10 g/cm², whereas the proton dosages decrease almost 30%.

It would appear that a higher-atomic-number material should be used behind the aluminum. This would increase the absorption of x rays. But such an observation is only qualitative and could be misleading if used for design. The higher-atomic-number material might increase the dosages if not preceded by the right amount of aluminum. Generally, an analysis of this type does not yield design information but indicates possible radiation hazard.

If this is indicated, then generally, for any given spacecraft weight, the design that surrounds the crew with the most uniform distribution of spacecraft materials will offer the best radiation protection. Thus, if at this point in the

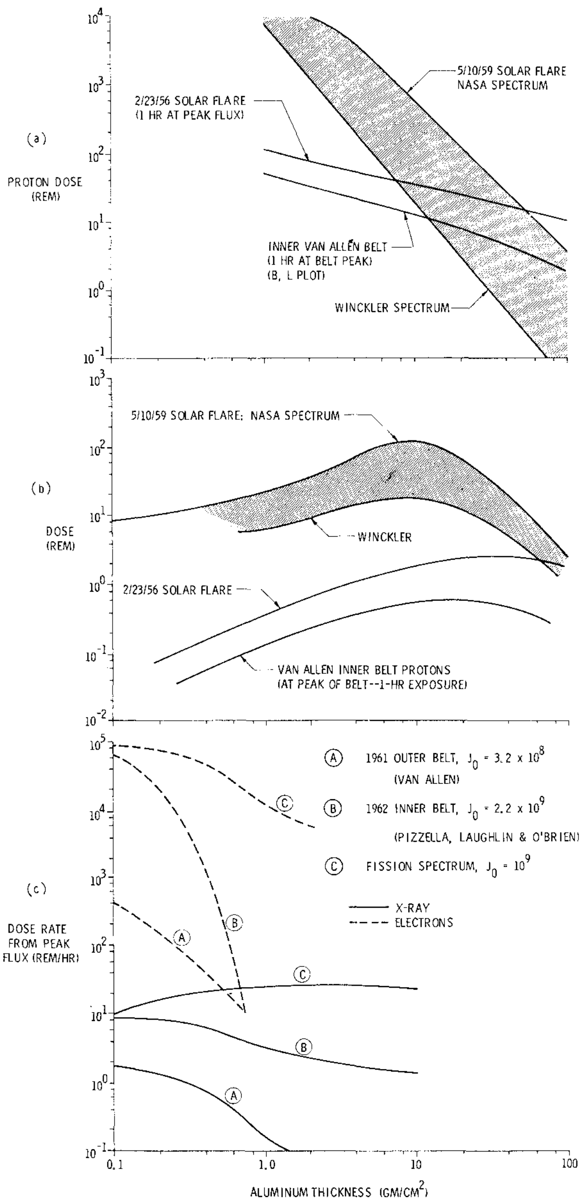

Fig. 1 Dose-absorber relationships: a) protons in space; b) neutron secondaries from space radiation protons; c) trapped electrons and their secondary x rays.

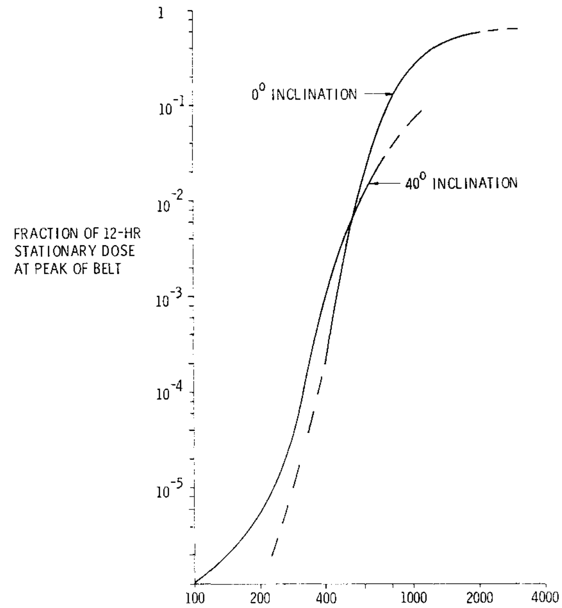

Fig. 2 Variation of geomagnetically trapped radiation dose with orbital altitude and inclination.

preliminary design there are some tradeoffs possible between propellants and heat shield—or between a localized or more uniformly distributed heat shield—high mission dosages would favor the distributed heat shield as more efficient than the other two designs. The results of this phase of the analysis may then affect the trajectories and configurations considered in the next phase.

Preliminary Design Studies

Initial Design Dosages

The next step is to determine the radiation dosages within the initial design. For this to be of more value than the first estimate, it is necessary to analyze the design in detail as to arrangement and composition of materials. Consider, for example, two adjacent equal-area sections of a space-

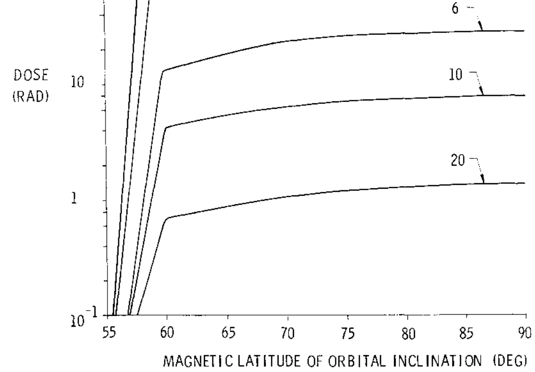

Fig. 3 Solar proton dosage as a function of orbital inclination for various absorber thicknesses for May 10, 1959 solar flare.

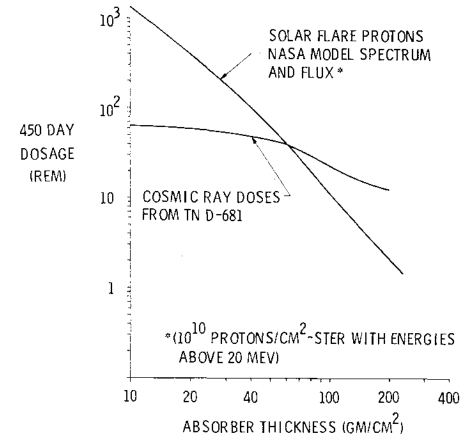

Fig. 4 450-day Mars mission dosages.

craft with net thicknesses of 0.2 and 1.0 g/cm², respectively. The sum of the Van Allen belt proton doses (Fig. 1a) passing through each of these sections is about 17% greater than the dose through the average thickness of 0.6 g/cm². This error depends on the degree of averaging and on the steepness of the dose vs absorber curve. It would thus be considerably larger for the May 1959 type of solar flare event than for either the protons of the Van Allen belt or the February 1956 type of solar flare.

Radiation dosages within an Apollo command module were evaluated.[2] The average vehicle thickness was 13.86 g/cm². Using this value to approximate the shielding effectiveness of the spacecraft gives dosages that are considerably lower than those determined using a multilayer, multisection analysis of the spacecraft. These factors are 5.41, 1.2, and 1.25, respectively, for the May flare event, the February flare event, and the inner belt protons. Other reasons for providing a detailed geometric analysis for the spacecraft can be seen from Table 2 for two early Apollo command modules.[4]

Although there are significant dosage differences between the two designs, a comparison made without evaluating the effects of inboard equipment would erroneously favor the second design. One should also not attempt to draw conclusions as to the types of design providing the better radiation protection—this was shown when an evaluation of another command module, similar in design to the L2C (aft-re-entering cone), gave a radiation dose lower than the first two, namely, 51 rad. The improvement came from a more extensive ablator on the cone walls, together with several other factors, none of which anticipated such a large decrease in dosage.

Another justification for the detailed geometric and composition analysis is that the dosage determinations do not provide inputs to design unless the dosage "hot spots" are located. Therefore, the dosage contribution from each spacecraft region must be available from the calculation in the form of dosage distribution maps.

Radiobiological and Physical Factors

Another important factor is that the human body is a complex, irregular target with varying absorption properties, radio sensitivities, and damage tolerances. The dosage values shown in the various figures have been entrance dosages. It is overconservative to consider these as whole-body dosages; this neglects self-shielding within the body which reduces the dosage as the radiation proceeds through the body. One approach to estimating whole-body radiation has been to assume a regular homogeneous shape, such as a water sphere, and to determine the dose at various depths which can be used to evaluate total absorbed radiation dose.

Aside from the errors introduced by the model, the advantages of using a regular shape are negated by the fact that the body entrance doses coming from the asymmetrical irregular spacecraft are not isotropic. Use of a more complex shape for the body model complicates the calculation considerably but does not offer extensive improvement unless the radiation anisotropy is included. However, efforts at improvement in whole-body dosage estimates are limited by the questionable usefulness of the whole-body dosage itself as the index of radiation damage.

The relative radiosensitivity and tolerance of different regions of the body have been considered in the recent development by NASA of a body model and a schedule of allowable dosages to different regions of the model. Although this model needs refinement, it represents a significant step toward better evaluation of the actual body damage.

The dosage calculations may now be set up using the body as an extension of the spacecraft, or vice versa, whichever gives the simplest geometry. We have no absolute measure of the accuracy as a function of analysis detail, but it would appear that as much as a factor of 5 in improved accuracy would result from a 400-section × 8-layer spacecraft representation vs a simple average. Another factor of 2 error might result from using a single absorber instead of the actual materials planned for the spacecraft. These calculations for a single combined spacecraft and body model might require 4 or 5 hr of IBM 7094 time for each dosage evaluation point.

Implicit in the analysis has been the availability of computational procedures[1, 2] to determine the interaction between the radiation particles (environment model) and matter (the spacecraft)—whether this is represented as a uniform spherical absorber or as a spacecraft of complex shape and composition. Therefore, because of the broad energy distributions of each of the space radiation constituents and the significance of secondary radiations, these computational procedures must be capable of accepting the environment model in great detail and following interactions through many very small increments of adsorber. As an example, consider the Van Allen belt electrons. If the inner belt were represented as a monoenergetic beam and if the passage through, say, 1 g/cm² were determined, using only one or two depth sections, then the resulting bremsstrahlung dosage estimate might not be more accurate than a factor of ±20.

Operational Factors

The feasibility study may show the hazard to be considerably reduced or eliminated by a modification of one or more of the operational factors. These include trajectory, mission duration, and date. An obvious modification to reduce the dosages shown in Table 1 would be to lower the orbital altitude. Choosing an orbital altitude of 400 miles would reduce the dosages by a factor of almost 100, as can be seen in Fig. 2.

To substantiate this effect, it is necessary to calculate the dosage using the complete mission time and the proper orbital elements. The Van Allen belts are irregular in shape. The effect of the irregularities is that the trapped radiation environment is not uniform in any one orbit and may also vary considerably among successive orbits.

For an extreme example, take a 100-naut-mile orbit injected at 0° latitude and 0° longitude, at an inclination of 40°. We found that no Van Allen belt protons were encountered until the middle of the seventh orbit. Then, in an interval of 2.7 min (Northeast of Madagascar) about 17.5% of the total 12-hr orbital dose would be received. The

Table 2 Proton dosages within command modules after flare of May 10, 1959[a]

Configuration	L2C, rad	M-1-1, rad
Neglecting CM equipment	1306	397
Including CM equipment	130	75

[a] Unprotected man, 18,099 rad.

remainder of the dose would be received over a period of 8.4 min as the satellite passed over Mozambique and Madagascar. The significance of the injection point and, in turn, the launch site is also apparent from this example.

In preparing the data used in Fig. 2, an attempt was made to smooth these irregularities by considering 12 hr as the unit of exposure time. This approximation would be poor for the case just discussed, since each of the next four or five orbits would probably encounter significantly higher particle fluxes as the orbit passed through the South Atlantic anomaly. Unless the complete mission is used in the calculation, it is doubtful whether the radiation flux for the mission can be obtained more accurately than within a factor of 2 or 3.

For the radiation constituents trapped in the geomagnetic field, these calculations would probably need about 1 hr of 7094 running time for every three days in orbit. It is desirable to preserve the dose (or flux) history in the calculations, so that the time and space locations of the high-radiation regions will be known. In the case just mentioned, the short exposure periods might suggest the use of a garment-like radiation shield to be inflated with water during intervals within the belt and later drained back into a reservoir. Small orbital maneuvers to avoid the edge of the belt might also be considered.

Cosmic-radiation intensity and solar-flare frequency vary inversely and directly, respectively, with the solar activity cycle. If the results of the preliminary radiation analysis during the feasibility studies showed these to be significant contributors to the mission dosage, then changes in the launch data could be examined to determine whether this is a practical means of reducing the hazard. On a Mars or Venus mission, the total dose from cosmic rays would become comparable to the solar-flare dose, as shown in Fig. 4. There might be little value in rescheduling the flight to a year of less solar activity, because the increase in dosage from cosmic radiation might more than offset the decrease in dosage from flare particles. Therefore, additional analysis would be indicated.

Preliminary Design Effort

Following these preliminary analyses, "firmer" values of configuration and/or mission will evolve. A more detailed radiation analysis can then be performed and fed back into the design groups At this point, some items may be "frozen," for example, the mission profile, but some gross features of the configuration may still be modified. The more detailed analysis, which provides dosage distribution maps, will be useful in formulating these modifications to be made in the preliminary design phase.

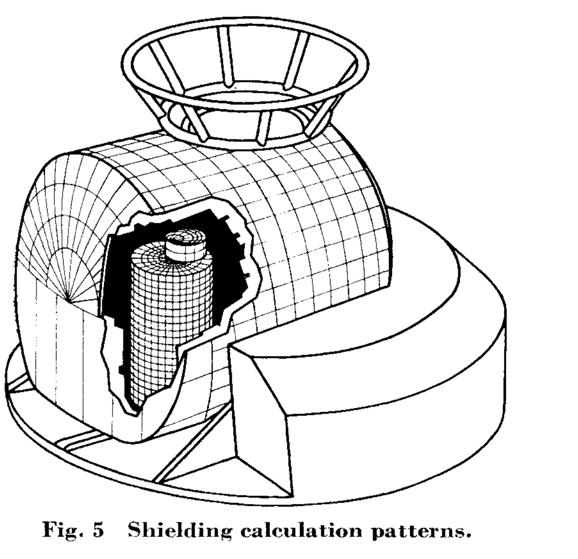

Fig. 5 Shielding calculation patterns.

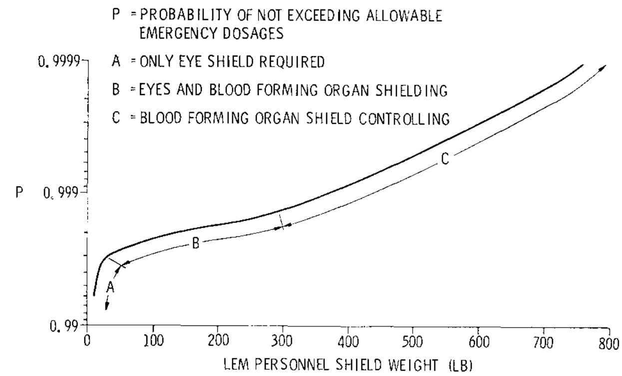

Fig. 6 Preliminary evaluation of LEM shielding requirements.

We recently completed a preliminary design analysis for a Lunar Excursion Module spacecraft, using the body model mentioned previously. Figure 5 shows the patterns used. The results, for the various doses in rad, were:

Average, inside the LEM (preliminary design; NASA model of the May 10, 1959 flare) 7456
Maximum, eye, 2020
Maximum, blood-forming organ, 133
Maximum, skin, 2814
Maximum, extremity, 9900

Note the nonuniformity of the doses and the fact that the maximum extremity dose was larger than the average entrance dose in the crew compartment.

Figure 6 shows the shield weights vs the probability of not exceeding the maximum allowable dosages for this spacecraft. The probabilities were derived from the environmental occurrence model. Shielding of each other by the two crewmen and shadow shielding by the moon were also considered in this analysis. Associated with this figure would be a set of dosage distribution charts which locate the dosage hot spots.

Design Effort

Figure 6 and its supporting data are the results of analyses performed during the preliminary design phase. Figures 7 and 8 represent an attempt to trace out the procedure during the main engineering design effort that would follow. This was done for the LEM mission, starting from the point at which a preliminary configuration has been evolved and using defined values of mission and payload. The radiation analysis effort has three major inputs; each requires improved or detailed values as the design effort proceeds. Input data format is indicated next, leading into preprocessing of the input for the dosage calculations which utilize the environment, the configuration, and the body models, and the radiation interaction models. The adequacy of our existing input preprocessing techniques is shown by the shaded box code.

To support the dosage calculations, an experimental check on the accuracy on the interaction model is available from irradiated sample test panels. If the dosage allowables are not exceeded, the next step is an experimental verification using more detailed spacecraft and body model sections. If the experimental checks do not support the analysis, then modifications to the spacecraft, body or interaction models are indicated in terms of the two-way connection, and the analysis is repeated with indicated modifications. If the allowables are exceeded and the experimental check is satisfactory, then a dosage alleviation study would be made (Fig. 8). Three categories of alleviation techniques are evaluated, considering alleviation relative to penalties that may be imposed elsewhere in the system. Some will be

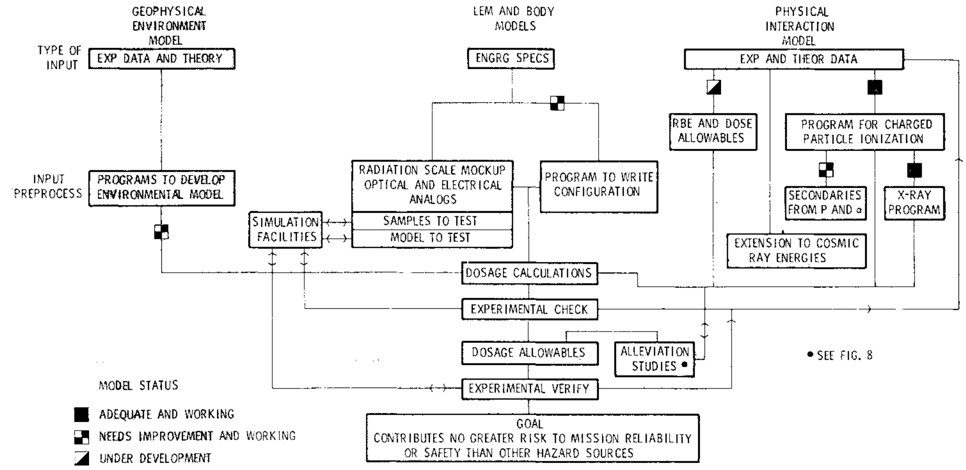

Fig. 7 Radiation analysis procedure.

found impractical or inefficient; one or more may offer considerable promise. The evaluation could require cooperation with many, if not all, of the project technical areas, with the government and with the contractor. For example, a possible alleviation technique may be removal of part of the command module shielding by the crewmen for use during the LEM portion of the mission.

Following the alleviation studies, the recommended technique (or techniques) can be implemented and the analysis procedure continued until the goal is reached.

Summary

Radiation shielding requirements are achieved "bootstrap" fashion in a series of feedback analyses. Inputs from various technical specialty areas, such as flight mechanics, structures, and configuration design, are used to help define the radiation hazard. The radiation analysis, in turn, furnishes data to these specialty areas for use in making modifications that will reduce the radiation dosages without adverse functional or operational effects.

Even a small amount of radiation shielding saved by the relocation of an already existing component is well worth the effort. In this regard, all of the components and materials of the spacecraft may be thought of as part of the radiation shield "subsystem." This subsystem is then designed, along with the other subsystems, so that specific shielding mass is kept to a minimum. Furthermore, if shielding is required, then proper provision for its storage or mounting can be made.

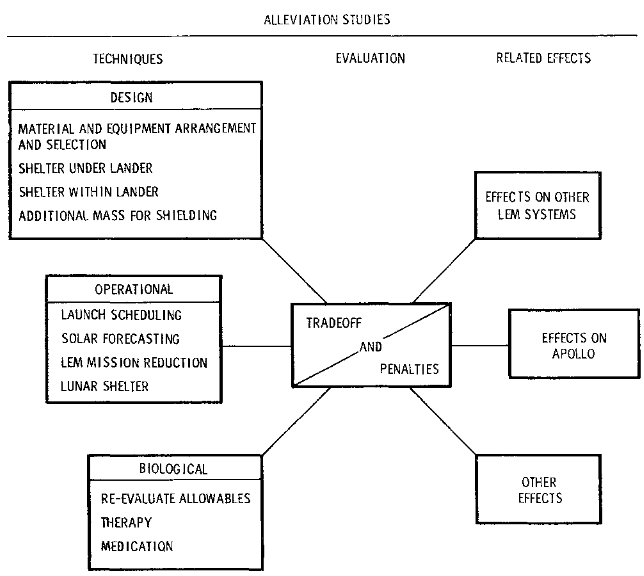

Fig. 8 Radiation analysis procedure.

This discussion implies that a high degree of systems integration capability must be available at the start of the preliminary design effort and that those performing that function need to recognize some of the problems and procedures of space radiation considerations.

Appendix: Space Radiation Environment

A satellite orbiting within the magnetosphere of the earth will encounter protons and electrons moving in an oscillatory North-South motion and drifting in longitude around the earth. These particles comprise the Van Allen belts. The size, shape, and variability of these belts have been well treated in the literature. The measurements made to date have shown regions of electrons and protons of the inner and outer belts.

The number vs energy distribution of inner-belt electrons or spectra at low altitudes as reported by members of the Van Allen group agrees well, in form, with estimates based on earlier measurements.[5] This spectrum, extrapolated to the peak flux altitude of the belt, is shown in Fig. 9. Also shown are the spectrum of electrons at the peak of the outer radiation belt and the fission electron spectrum believed to be representative of the peak of the artificial radiation belt created by the Starfish high-altitude nuclear explosion. A flux contour chart of the natural electrons at one longitude is shown in Fig. 10. It should be noted that, due to asymmetries of the magnetic field, this cross section is not constant at all longitudes.

In passing through matter, say, the walls of a spacecraft, some of the energy of the electrons goes into the creation of gamma rays from the nucleus of the absorbing material. These bremsstrahlung gamma rays must also be considered part of the radiation dosages that result from the Van Allen belt electrons. High-energy protons of the inner Van Allen belt are another radiation constituent. Their flux contours are plotted in the B, L magnetic field coordinate system of McIlwain[6] in Fig. 11. The electrons of the artificial radiation belt are also plotted in the same coordinates.[7]

The differential energy spectrum of the inner-belt protons at the peak of the belt is given by

$$dN = 0.117\ \mathrm{KE}^{-0.742}\, dEd\Omega \qquad 10 < E < 56.5 \text{ Mev}$$
$$dN_2 = 0.808\ \mathrm{KE}^{-1.22}\, dEd\Omega \qquad 56.5 < E < 130$$
$$dN_3 = 4.39\ \mathrm{KE}^{-1.57}\, dEd\Omega \qquad 130 < E < 320$$
$$dN_4 = 52.4\ \mathrm{KE}^{-2.00}\, dEd\Omega \qquad 320 < E < 700$$

where $K = 6600\ \mathrm{cm}^{-2}\ \mathrm{sec}^{-1}\ \mathrm{ster}^{-1}$.

High-energy protons emitted during solar flares are another radiation constituent. The intensity, frequency, duration, and return periods for these events are not yet adequately known. It is known that the course of a flare event is de-

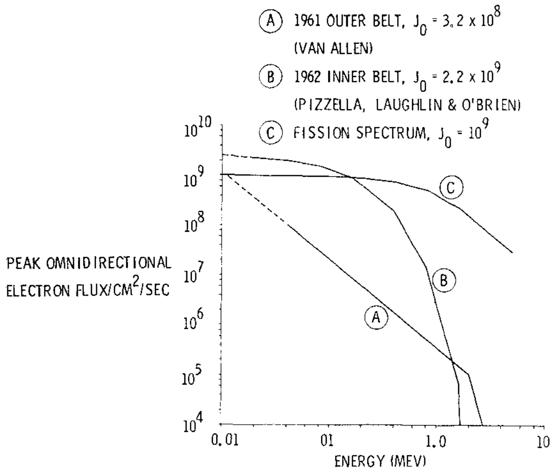

Fig. 9 Integral electron kinetic-energy spectra.

pendent upon the intensity of the flare itself, the preconditioning of interplanetary space by the variable lower-energy solar plasma, and the geometry between the sun and the place of measurement. The presence of the geomagnetic field also influences the course of the event in the vicinity of the earth.

Therefore, flare events as measured near earth have shown differences in intensity by many orders of magnitude. As a result of the rather complex occurrence model and the poor statistics to date, the procedure for considering flare events has been to select one or more design events, from the most severe recorded, to represent the conditions to be expected. Three such design events are February 23, 1956, and two versions of the May 10, 1959 flare. The first is derived from Foelsche's plot,[8] and the other two are derived from Winckler's[3] observations and from a later NASA version suggested for use in Project Apollo at one time.

The differential kinetic energy spectra for the events are shown below:

$$dN_1 = 2.563 \times 10^{-1}\ KE^{-1.2985}\ dEd\Omega \qquad 0.60 < E < 130 \text{ Mev}$$

$$dN_2 = 7.859 \times 10^{-1}\ KE^{-1.4460}\ dEd\Omega \qquad 130 < E < 550$$

$$dN_3 = 2.957 \times 10^{3}\ KE^{-2.5520}\ dEd\Omega \qquad 550 < E < 1600$$

$$dN_4 = 6.961 \times 10^{11}\ KE^{-5.040}\ dEd\Omega \qquad 1600 < E < 5000$$

$$dN_5 = 2.802 \times 10^{22}\ KE^{-7.850}\ dEd\Omega \qquad 5000 < E < 10{,}000$$

where

$$K = 5.0 \times 10^4 \text{ protons/cm}^2\text{-sec-ster} \qquad \text{(A1)}$$

$$dN = 9.390 \times 10^9\ E^{-4.8}\ dEd\Omega \qquad 20 < E < 10{,}000 \text{ Mev} \qquad \text{(A2)}$$

$$dN_1 = 6.268\ KE^{\,2.07}\ dEd\Omega \qquad 5 < E < 60$$

$$dN_2 = 1.376 \times 10^4\ KE^{-3.95}\ dEd\Omega \qquad 60 < E < 10{,}000 \qquad \text{(A3)}$$

where $K = 3.988 \times 10^{10}$ protons/cm²-ster.

The first spectrum was assumed to represent the peak flux which decayed as t^{-2} (with t in hr). The second spectrum was measured about 29 hr after the beginning of the event. We assume that this spectrum constant for 30 hr describes the complete event. The third spectrum is already time integrated.

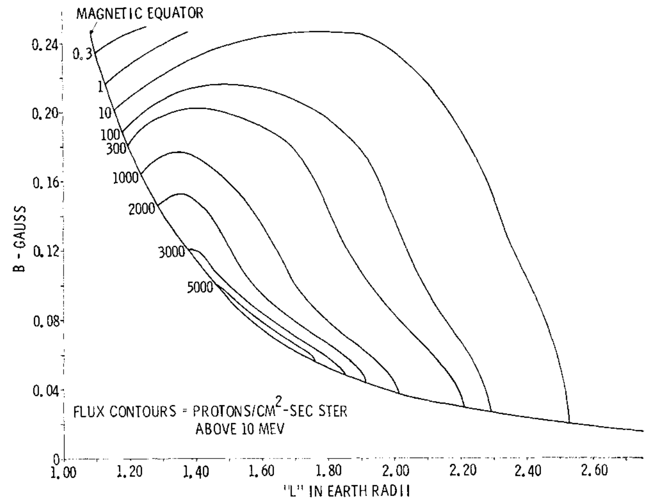

Fig. 10 Flux of electrons at one longitude in the Van Allen belts.

The next constituent is cosmic radiation, consisting primarily of high-energy protons and alpha particles but also including significant amounts of nuclei of heavier elements. The equation of the cosmic radiation flux is given by Winckler in Ref. 9 as

$$N\ (>E) = 0.3\ (1 + E)^{-1.5} \qquad 5 \times 10^8 < E \text{ Mev}$$

Knowledge of the space radiation environment has improved greatly in the last three years. There have been significant revisions in models of the intensity of the trapped radiation, with correspondingly significant changes in the associated hazard.[10] Recent measurements have shown a large flux of high-energy protons in the outer Van Allen belt.[11] These must be included in the environmental model for space missions in high-inclination trajectories or in orbital altitudes exceeding about 4000 miles. It is quite likely that, as we continue our measurement programs, addi-

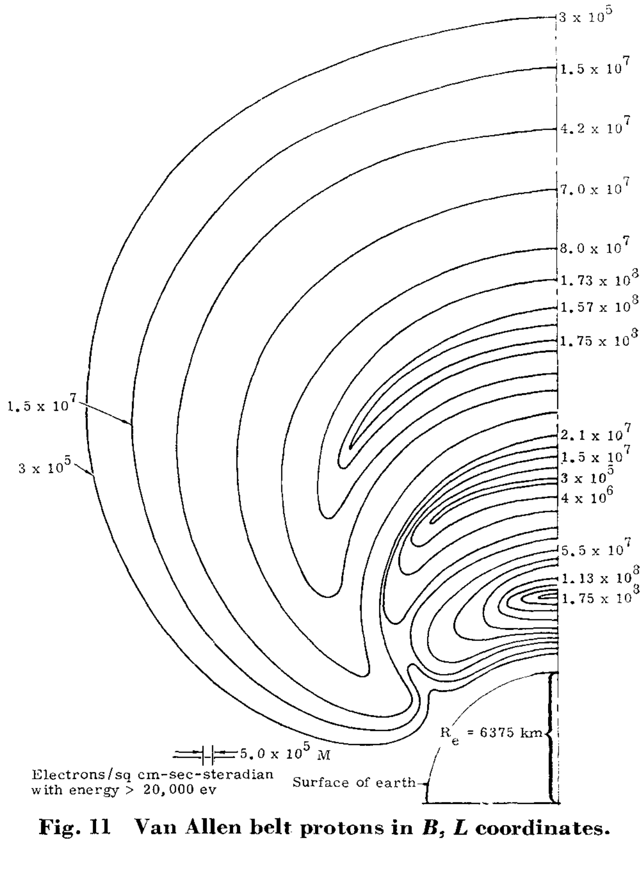

Fig. 11 Van Allen belt protons in *B*, *L* coordinates.

tional changes will be made in the models. Some of these changes will show more detailed distributions of flux and energy distribution, some will correct ambiguities and errors in earlier measurements, and other changes will reflect the dynamic nature of the space radiation environment as, for example, the variations associated with the sunspot cycle.

References

[1] Beck, A. J., Divita, E., and Russak, S. L., "Evaluation of space radiation safety procedures in the design and operation of some early manned lunar vehicles," *Proceedings of the Sixth Symposium on Ballistic Missile and Aerospace Technology* (Academic Press, New York, 1961), Vol. 3, pp. 365–426.

[2] Beck, A. J. and Divita, E. L., "Evaluation of space radiation doses received within a typical spacecraft," ARS J. **32**, 1668–1676 (1962).

[3] Winckler, J. R. and Bhavsar, P. D., "Low-energy solar cosmic rays and the geomagnetic storm of May 12, 1959," J. Geophys. Res. **65**, 2637–2656 (1960).

[4] Russak, S., "Designing for space radiation," Aerospace Eng. **21**, 60–81 (1962).

[5] Pizzella, G., Laughlin, C. D., and O'Brien, B. J., "Note on the electron energy spectrum in the inner Van Allen belt," J. Geophys. Res. **67**, 3281–3287 (1962).

[6] McIlwain, C. E., "Coordinates for mapping the distribution of magnetically trapped particles," J. Geophys. Res. **66**, 3681–3691 (1961).

[7] Hess, W. N., "The artificial radiation belt made on July 9, 1962," J. Geophys. Res. **68**, 667–683 (1963).

[8] Foelsche, T., "Protection against solar flare protons," Paper no. 61-34, 7th Annual Meeting of American Astronautical Society, Dallas, Tex. (January 1961).

[9] Jacobs, G. C., *Proceedings of Conference on Radiation Problems in Manned Space Flight* (Government Printing Office, Washington, D. C., 1960), NASA TN D-588.

[10] Russak, S. L., "Radiation dosages from electrons and bremsstrahlung in the Van Allen Belts," *Proceedings of the Symposium on Protection Against Radiation Hazards in Space, Gatlinburg, Tennessee* (US Atomic Energy Commission, Oak Ridge, Tenn., 1962), pp. 760–772.

[11] McIlwain, C. E., "The radiation belts, natural and artificial," Science **142**, 355–361 (1963).